Green light emission in aluminum oxide powders doped with different terbium concentrations

L. Mariscal-Becerra[a,*], S. Carmona-Téllez[b], R. Vázquez-Arreguín[c], C.M. García-Rosas[d],
C. Falcony[a], H. Murrieta[b], and M.A. Sánchez-Alejo[b]

[a]*Centro de Investigación y de Estudios Avanzados del Instituto Politécnico Nacional,*
Gustavo A. Madero, México D.F. 07360, México.
e-mail: mariscal2005@gmail.com
[b]*Instituto de Física, Universidad Nacional Autónoma de México,*
Coyoacán, México D.F. 04510, México.
[c]*Escuela Superior de Cómputo, Instituto Politécnico Nacional,*
Del. Gustavo A. Madero. México
[d]*Ciencias, Universidad Nacional Autónoma de México,*
Coyoacán, México D.F. 04510, México.

Different emission intensities presented in aluminum oxide phosphors corresponding to different concentrations of doping performed with terbium are analyzed. The phosphors were synthesized by the evaporation technique and were characterized by photo and cathodoluminescence, x-ray diffraction, and EDS techniques for different incorporation percentages of terbium as dopant; they show characteristic transitions in 494, 543, 587 and 622 nm, corresponding to $^5D_4 \rightarrow \,^7F_6$, $^5D_4 \rightarrow \,^7F_5$, $^5D_4 \rightarrow \,^7F_4$ and $^5D_4 \rightarrow \,^7F_3$, respectively when they are excited with $\lambda_{\mathrm{exc}} = 380$ nm wavelength at room temperature. The results of XRD show the presence of α-Al_2O_3 phases with peaks located at $2\theta = 25.78$, 35.34, 37.96, 43.56, 45.8, 52.74, 57.7, 61.5, 66.74, 68.44, 77.12 and 80.94, and the δ-Al_2O_3 phase $2\theta = 32.82$, 45.8, 61.36 and 66.74. These compounds were heat treated for two hours at $1100°$C. EDS analyzes indicate that these compounds have close to 60% oxygen around of 40% aluminum in the presence of terbium as dopant which indicates a stoichiometry close to the expected one for alumina.

Keywords: Terbium; luminescence; powders; aluminum oxide.

PACS: 78.55.Qr; 81.05.Rm; 81.20.Ka

1. Introduction

The compounds of aluminum oxide doped with different elements like Europium [1], Manganese, Cerium [2], Lanthanum [3], Erbium, Praseodymium [4], Terbium [5], Iron, Chromium [6], Carbon [7], Ytterbium [8] and Thulium [9] have been studied carefully because of its excellent physical and chemical properties, such as luminescence, hardness, resistance to ionizing and thermal radiation, high dielectric constant and insulating characteristics. That's why they can be applied as dielectric materials with high refractive index and a wide bandgap, and in the field of optical coatings and metal-oxide semiconductor devices for next generation devices; those are just a few reasons why alumina has a large potential for its wide variety of applications.

The compounds of aluminum oxide doped with rare earths are obtained by different techniques such as spray pyrolysis [2,5], organic acids combustion [3], sol-gel [4,8], pulverizing-metallurgy [6], laser ablation sputtering [10,11], dissolvent evaporation [1] and other more [12-17]. These have been developed for the various compounds Al_2O_3 that are doped in simple experimental conditions. Oxides doped with rare earths are of the most promising; because the 4f orbitals are protected very effectively by the electrons of the 5s2 5p6 outer layers, this is why the states originating from the different configurations 4f^n are only slightly affected by

the surrounding ions and remain virtually unchanged for an specific ion in all its compounds, according to this electronic configuration, f-f transitions have narrow and sharp peaks observed in the optical absorption and emission spectra.

The Al_2O_3 is a material with a great technological importance due to its optical transparency from the ultraviolet to the near infrared; and its excellent mechanical properties and chemical stability, presenting different crystalline phases at different temperatures; the phase α-Al_2O_3 being the most stable.

In this work optical, structural and morphological characteristics of aluminum oxide powders doped with different concentrations of terbium chloride are presented; the samples were obtained through simple evaporation technique at a temperature of $1100°$C to obtain a luminescent material in the green region of the spectra.

2. Materials and Methods

The aluminum oxide Al_2O_3 powders doped with different percentages of $TbCl_3$ were obtained through the evaporation technique [1]. The solution was obtained by dissolving in 5 ml of deionized water (18 MΩ cm^{-1}), an appropriate quantity of $Al(NO_3)_3$ and $TbCl_3$ to (3, 5, 7, 10, 12 and 15 at. %). Each of the compounds were dried at $200°$C and subsequently calcined at $1100°$C for two hours and tem-

pered at room temperature; its structure was analyzed by X-ray diffraction (XRD) using a Siemens D5000 diffractometer with 1,540Å (Cu Kα) operating at 30 keV; the chemical composition of the powders was measured using energy dispersive spectroscopy (EDS) with a model Leica Cambridge Stereoscan 440 Electron Microscope equipped with an X-ray detector with beryllium window. The luminescent spectra were obtained with a Perkin-Elmer LS-50B; Photoluminicence (PL) emission spectra were obtained using a continuous λ_{exc} = 380 nm wavelength using a UV 8W mercury lamp, model UVGL-25; cathodoluminescence (CL) measurements were performed in a stainless steel vacuum chamber with a cold cathode electron gun (Luminoscope, model ELM-2 MCA, RELION Co.). Powders were placed inside the vacuum chamber and evacuated to $\sim 10^{-2}$ Torr. The electron beam was deflected through a 90° angle to focus onto the luminescent film normal to the surface; the diameter of the electron beam on the powders was 3 mm approximately. The emitted light was collected by an optical fiber and fed into a SPEX Fluoro-Max-P spectrophotometer. All measurements were carried out at room temperature.

3. Results and discussion

The crystal structure of the powders was analyzed by X-ray diffraction (XRD)Show in Fig. 1 are the diffraction plot of Al$_2$O$_3$:Tb^{3+} phosphors. Previous studies have shown that various crystalline phases are present in Al2O3 compounds, these phases α-Al$_2$O$_3$, γ-Al$_2$O$_3$ and δ-Al$_2$O$_3$ appear when this compound has been thermally treated from 800°C to 1000°C, whereas phase α-Al$_2$O$_3$ occurs at temperatures above 1000 to 1200°C [19] The graph shows that powders Al$_2$O$_3$:Tb^{3+} have the crystal phase α-Al$_2$O$_3$ with peaks located at 2Θ = 25.78, 35.34, 37.96, 43.56, 45.8, 52.74, 57.7,
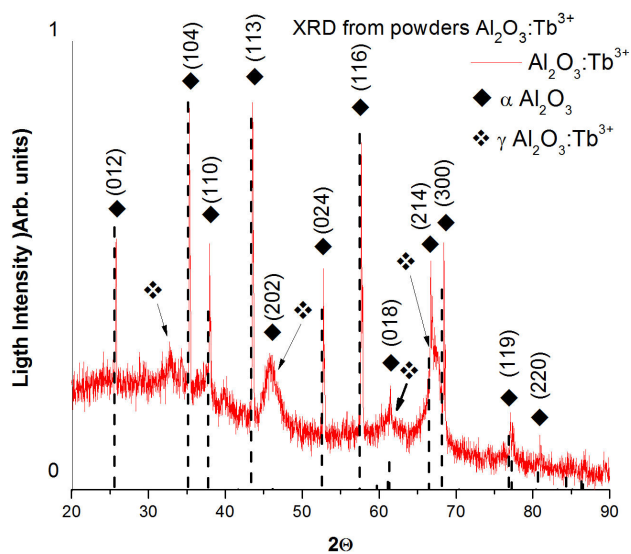

FIGURA 1. XRD measurements from Al$_2$O$_3$:Tb^{3+} synthesized at 1100°C and data of JCPDS card 81-1667. The card data are plot in dash line.

61.5, 66.74, 68.44, 77.12 and 80.94, which are associated with the planes (012), (104), (110), (113), (202), (024), (116), (018), (214), (300), (119) and (220), according to diffraction JCPDS card 81-1667. The α-Al$_2$O$_3$ phase is a hexagonal primitive cell [19,20], with lattice parameters a = b = 4.75999 Å c =12 .99 481 Å [21]. In this compound are also identified peaks corresponding to the phase α-Al$_2$O$_3$, in 2Θ = 32.82, 45.8, 61.36 and 66.74, associated with the planes (220), (400), (511) and (440) according to JCPS card 50-0741, this phase is cubic with lattice parameter a =7.939 Å.

The crystal size was estimated by Sherrer's formula [22]:

$$T = \frac{0.9\lambda}{B \sin \theta_B} \tag{1}$$

Where, T represents the crystal size, λ is the wavelength radiation CuKα (1.5406 Å), B is the half width of the diffraction peak and θ_B the Bragg's angle measured in radians; sizes calculated for the phase δ-Al$_2$O$_3$, is 32.47 nm in θ = 32.72, in θ = 37.88 its size is of 40.33 nm, at θ = 45.8 its value is 20.8 nm, at θ = 61.48 is 26.3 nm, at θ = 66.64 is 17.98 nm and at θ = 77.1 is 22.22 nm [23]. It is important to note, that no significant differences in the XRD patterns among powders Al$_2$O$_3$ and those doped with Tb^{3+} are detected, probably due to the low percentage of terbium; because of this it is not surprising that there are not large clear differences between Al$_2$O$_3$ powders and α-Al$_2$O$_3$ phase doped with terbium. The EDS measurements indicate the presence of aluminum, oxygen and a minimum part of terbium, EDS results are shown in Table I, in the table the results of the powders correspond to 12 at. % of doped with terbium.

Even though EDS is not a quantitative technique it is useful to estimate the chemical composition of samples, EDS measurements on doped and non-doped phosphors were performed and the results are listed in Table I. In the case of doped samples, it is shown just the 12 at. % of Tb, because is which has the highest luminescent intensity. According to the expected stoichiometry for aluminum oxide (a relation of 3 to 2 of the oxygen to aluminum), a presence of 60% of oxygen and 40% of aluminum, is observed. In the case of doped samples, there is an apparent substitution of Al ions by Tb^{3+}, but in a low quantity, this effect is observed in some previous reports in some host materials, techniques and dopants [3,18,20,23].

TABLE I. Measurement of percentage and weight of aluminum, oxygen and terbium for EDS the phosphors Al$_2$O$_3$ and Al$_2$O$_3$:Tb^{3+} at 12% doped.

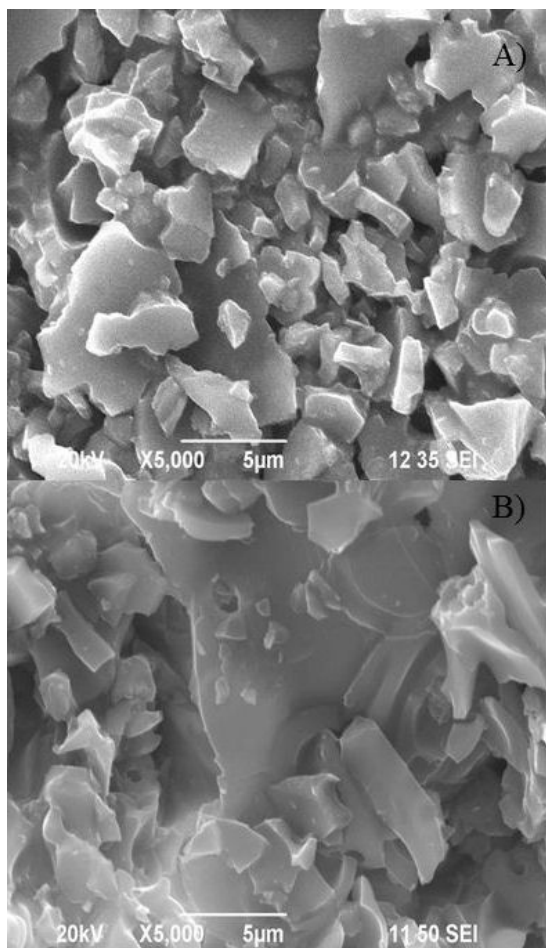| Al$_2$O$_3$			Al$_2$O$_3$:Tb^{3+}		
Element	weight %	atomic %	Element	weight%	atomic%
O	49.59	62.39	O	43.60	60.00
Al	50.41	37.61	Al	47.51	38.76
Tb	—–	—–	Tb	8.89	1.24
Total	100.00		Total	100.00	

FIGURA 2. A) High resolution SEM of Al2O3 undoped powders, B) High resolution SEM of Al_2O_3:Tb^{3+} powders.

FIGURA 3. Luminescence intensity as a function of Tb^{3+} ion concentration into Al_2O_3:Tb^{3+} powders.
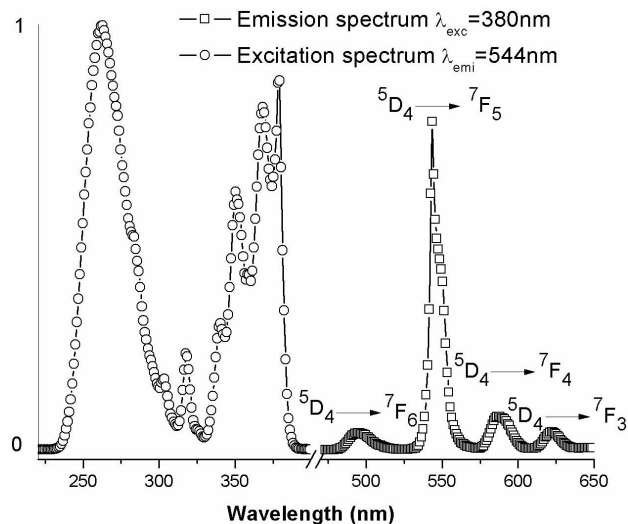
FIGURA 4. Comparison between emission and excitation spectrum for Al_2O_3:Tb^{3+} phosphors.

Figure 2 shows two SEM images of Al_2O_3 and Al_2O_3:Tb^{3+} phosphors annealed at 1100°C, it can be observed that the powder particles grow in a sheet form, and have the formation of agglomerates of our material with various sizes (between 300 nm to 5 microns) , although smaller powder sizes of about 100 nm are also observed. The size is determined, largely, by the grinding process of the powders. No difference in size or morphology was found between doped and none-doped powders. These micron-sized powders are particularly good for various technological applications like lighting devices.

The normalized emission spectra were obtained for the aluminum oxide powders doped with percentages from 3 at. % to 15 at. % of terbium and are shown in Fig. 3. In the graph are shown transitions for the Tb^{3+} ion, which appear at 494, 543, 587 and 622 nm and corresponding to $^5D_4 \rightarrow {}^7F_6$, $^5D_4 \rightarrow {}^7F_5$, $^5D_4 \rightarrow {}^7F_4$ and $^5D_4 \rightarrow {}^7F_3$ [2,5,17,18]; respectively, using a continuous excitation radiation of 380 nm wavelength at room temperature, The dominant peak for these spectra is the one associated with the transition $^5D_4$ to $^7F_5$ at 544 nm, which gives the characteristic green light emission identified with the presence of Tb^{3+} ions. The emission intensity for different terbium doping concentra-
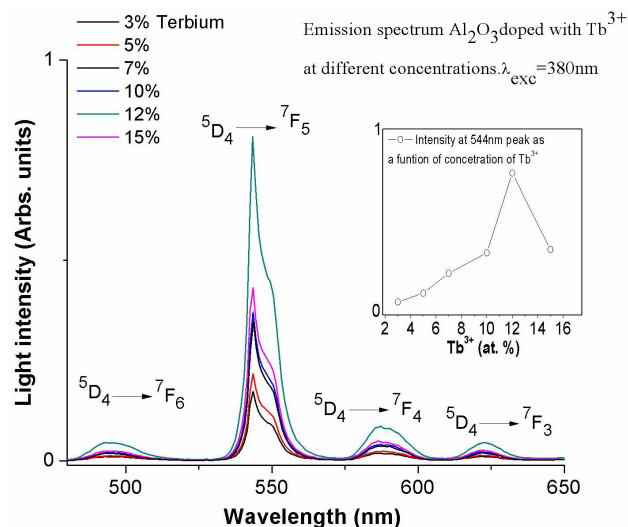
tions are shown in Fig. 3 indicating that this is increased by the increase of doping percentage, the best efficiency is presented with the percentage of 12 at. % is presented the best efficiency, while 14 at. % dopant diminishes in intensity because they present quenching effect associated with energy transfer among dopant ions.

In Fig. 4 the excitation and emission spectra are shown, in the excitation spectra are observed that exist some peaks capable to excite Tb^{3+} ions, the higher peaks that could excite are 260 and 380 nm; the broad excitation band centered at 260 nm, is commonly ascribed to the O-Tb charge-transfer transition (ligand to metal charge transfer). the general behavior of these results is similar to that reported previously in which a dependence of the photoluminescence intensity is correlated with the incorporation efficiency of the Tb ions into the aluminum oxide matrix; all of them show a band of
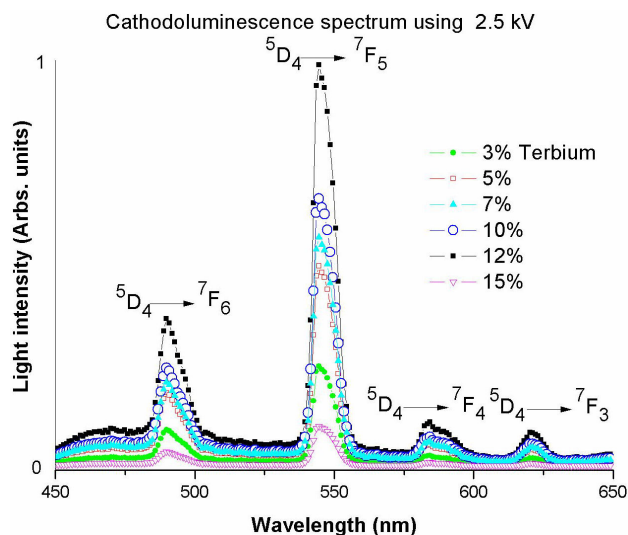
FIGURA 5. CL emission spectra intensity as a function of Tb^{3+} ion concentration into Al_2O_3:Tb^{3+} powders.
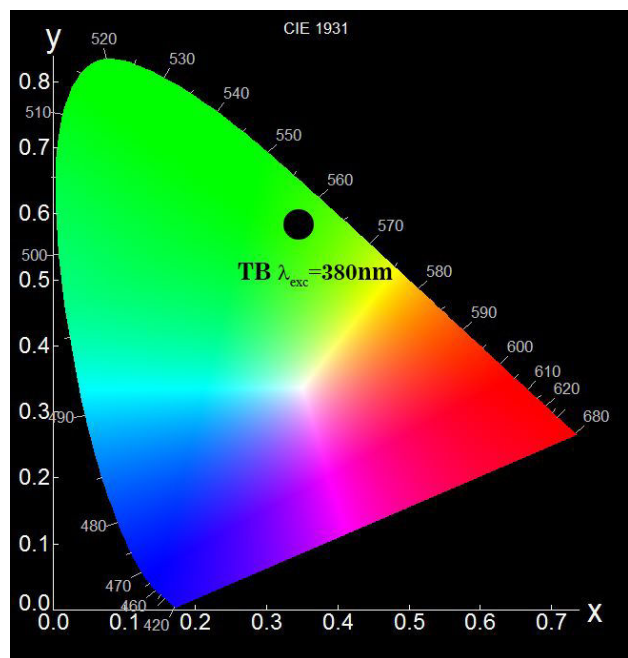

FIGURA 6. CIE diagram Al_2O_3:Tb^{3+} powders.

high intensity at 260 nm, additionally the Al_2O_3:Tb^{3+} powder spectrum presents other peaks at 303, 318, 340, 350, 368, 368 and 380 nm. The intensity in 260 nm is significantly more intense than the forbidden transitions centered at 303 nm ($^5I_8 \rightarrow {}^7F_6$, $^5F_4$, $^5F_5$, $^5H_4$), 318 nm ($^7F_6 \rightarrow {}^5H_5$, $^5H_6$), 340 nm ($^7F_6 \rightarrow {}^5H_7$, $^5D_1$), 350 nm ($^5L_78 \rightarrow {}^7F_6$, $^5G_3$), 368 nm ($^7F_6 \rightarrow {}^5L_9$, $^5D_2$, $^5G_5$) and 380 nm ($^7F_6 \rightarrow {}^5L_{10}$, $^5G_6$, $^5D_3$), as can be seen in the Fig. 4, which describes the charge-transfer transition that occurs between the ligand and the metal (O-Al), the most luminescent intensity with 12 at. % of Tb^{3+} in the powders of Al_2O_3:Tb^{3+}, those phosphors have high quantum yield efficiency about 25.97. The fluores-

cence quantum yield is defined as the ratio of the number of photons emitted to the number of photons absorbed [23].

Figure 5 shows the CL spectrum of Al_2O_3:Tb^{3+} powders, during CL measurements the anode voltage and the beam current were kept constant. The spectrum consist of a number of well resolved peaks at 490, 544, 590, and 622 nm, which are assigned to $^5D_4$ to $^7F_6$, $^7F_5$, $^7F_4$ and $^7F_3$, of the Tb^{3+} ion transitions respectively. The most intense emission occurs at 544 nm and is due to $^5D_4$ to $^7F_5$ transition. Similar results have been obtained earlier for oxide doped with Tb^{3+}, and the results are consistent with those previously mentioned [3,18,24], cathodoluminescence results obtained from all the used concentrations of terbium as dopant, are consistent with the photoluminescence when they were excited using continuous 380 nm wavelength radiation having its maximum at 12 at. %.

Figure 6 shows the CIE diagram (Commission International de l' éclairage) [25] which defines the three primary colors of color displays, and from these the combination of different colors is obtained to generate secondary colors in its different shades, depending on their individual coordinates (x, y). For Al_2O_3:Tb^{3+} powders, when excited with 380 nm, the coordinates are ($x = 0.31$, $y = 0.5111$), according to the CIE diagram, they are located in the green color, being these results comparable to previous ones reported for Tb^{3+} in a variety of different hosts [2,3,16].

4. Conclusion

Analysis of the aluminum oxide powder doped with terbium in different concentrations indicates from the results of X-ray diffraction that these powders are polycrystalline and that phase α-Al_2O_3 peaks located at observed $2\Theta = 25.78$, 35.34, 37.96, 43.56, 45.8, 52.74, 57.7, 61.5, 66.74, 68.44, 77.12 and 80.94, and phase α-Al_2O_3, in $2\Theta = 32.82$, 45.8, 61.36 and 66.74 are present. The photoluminescence spectrum shows that is associated with terbium transitions and better emission efficiency occurs when is used 12 at. % of dopant; these phosphors have a quantum yield efficiency around 25.97, using a continuous 380 nm wavelength as excitation radiation, this wavelength is of less energy than 260 nm wavelength, which is commonly used in previous reports; therefore if could get low cost LEDs for green light; CL results also show that the transitions are associated with Tb^{3+} ion. EDS analysis shows that aluminum oxide corresponds to the stoichiometric formula Al_2O_3, due to these results it can be considered that this type of compound is a good candidate to have green light and its preparation is simple and of low economic cost.

Acknowledgments

1. J. Azorín, A. Esparza, C. Falcony, T. Rivera, M. García and E. Martínez, *Radiation Protection Dosimetry* **100** (2002) 277-279.

2. R. Martínez-Martínez, E. Yescas, E. Álvarez, C. Falcony, U. Caldiño, *Advances in Science and Technology* **82** (2013) 19-24.

3. S.J. Yoona, S.J.Dhobleb, K.Parka, *Ceramics International* **40** (2014) 4345-4350.

4. A.A. Kaplyanskiĩ, A.B. Kulinkin, A.B. Kutsenko, S.P. Feofilov, R.I. Zakharchenya, and T.N. Vasilevskaya, *Physics of the solid state* **40** (1998).

5. S. Carmona Téllez, C. Falcony, M. Aguilar Frutis, G. Alarcón Flores, M. García Hipólito, and R. Martínez Martínez, *ECS Journal of Solid State Science and Technology*, **2** (2013) R111-R115.

6. Saidatulakmar Shamsuddin, Shamsul Baharin Jamaludin, Zuhailawati Hussain and Zainal Arifin Ahmad, *Journal of Physical Science* **19** (2008) 89-95.

7. W.M. de Azevedo, G.B. de Oliveira, E.F. da Silva Jr, H.J. Khoury and E.F. Oliveira de Jesus, *Radiation Protection Dosimetry* **119** (2006) 201-20.

8. J.K. Krebs and U. Happek, *Journal of Luminescence* **94-95** (2001) 65-68.

9. V.S.M. Barros, W.M. de Azevedo, H.J. Khoury, M.E.A. Andrade, P. Linhares Filho, *Radiation Measurements* **45** (2010) 435-437.

10. L.A Stone, H.V Snelling and A.G Jenner, **109-110** (1997) 389-392.

11. P. Jin, G. XU, K. Yoshimura, J. Alami and U. Helmersson, *Template Journal of Vacuum Science & Technology A* **20** (2002) 2134.

12. Y. Kim, S.M. Lee, C.S. Park, S.I. Lee and M. Y. Lee, *Applied Physics Letters* **71** (1997) 3604.

13. D. Barreca, Giovanni A. Battiston, R. Gerbasi and E. Tondello, *J. Mater. Chem.* **10** (2000) 2127-2130.

14. X.Y. Chen, L. Yang, R.E. Cook, S. Skanthakumar, D. Shi and G. K. Liu, *Nanotechnology* **14** (2003) 670-674.

15. F. Wiest *et al.*, *Thin Solid Films* **496** (2006) 240-246.

16. Fei Lu, R. Carius, A.A. Alam and M. Heuken, *Journal of the Korean Physical Society* **46** (2005) S48-S51.

17. A. Gedanken, R. Reisfeld, L. Sominski, Z. Zhong, Yu. Koltypin, *Applied physics letters* **77** (2000) 14.

18. J.V. Soares, C.F. Gugliotti, Y.S. Kawashima, S.H. Tatumi, J.C.R. Mittani, *Radiation Measurements* (2014).

19. G.N. Darriba, R. Faccio, M. Rentería, *Physica B: Condensed Matter* **407** (2012) 3093-3095.

20. Yu-Chen Lee, Shaw-Bing Wen, Liang Wenglin and Chih-Peng Lin, *J. Am. Ceram. Soc.* **90** (2007) 6; **90** (2007) 1723-1727.

21. F. Izumi, H. Asano, H. Murata and N. Watanabe, *J. Appl. Cryst.* **20** (1987) 5.

22. B.D. Cullit, S.R. Stock, *Elements of X-Ray Diffraction*, (Prentice-Hall Inc., 2001) p. 388.

23. Lakowicz, Joseph R. *Principles of Fluorescence Spectroscopy* (Kluwer Academic / Plenum Publishers 1999) p.10. ISBN 978-0-387-31278-1.

24. E.H. Penilla, Yasuhiro Kodera, and J.E. Garay, *Adv. Funct. Mater.* **23** (2013) 6036-6043.

25. D.B. Judd *et al.*, *Journal of Optical Society of America* **54** (1964) 1031.